



Soft X-ray Absorption and Resonant Scattering at ALBA synchrotron

BOREAS - BL29
Beamline Of REsonant
Absortion and Scattering

P. Gargiani – ALBA workshop 13 November 2014



- BL scientific case
- Basic overview of the technique
- BOREAS endstations overview
- Example results/applications



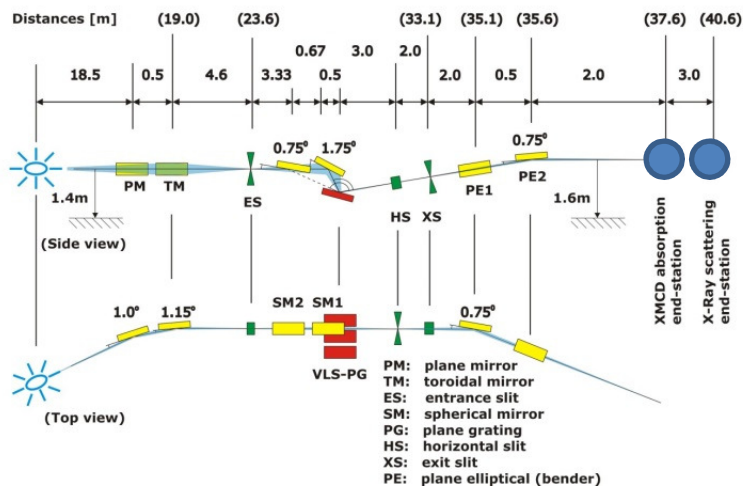
> Apple II undulator (full polarization control) + VLS grating mono → 80-**4500** eV energy range

> **2 endstations** : XAS/XLD/XMCD cryomagnet & RXS chamber + **2 T magnet**

Scientific case

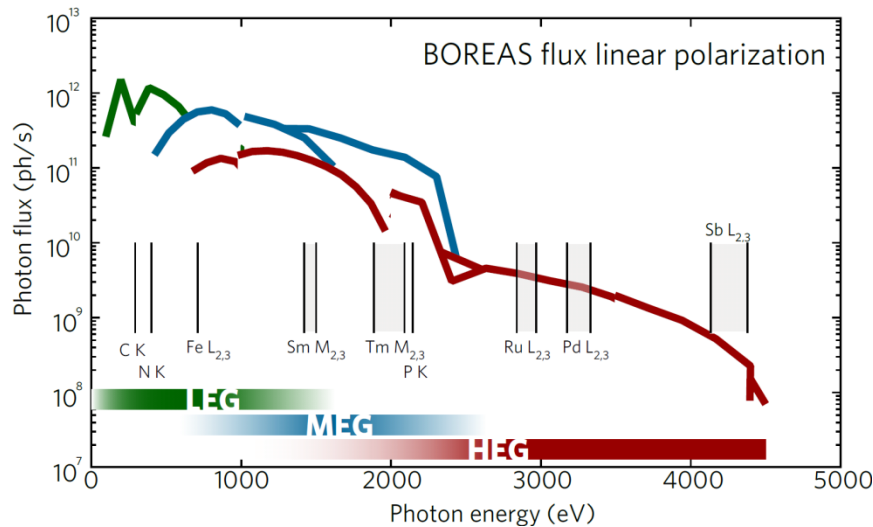
> HECTOR: Cryomagnet up to 6 T (2 T in **sphere mode**) with sample preparation chamber

> MARES: Resonant soft X-ray scattering chamber with in-vacuum detectors sample prep. chamber and in-situ deposition possibility (metal/organic evap) (endstation under commissioning)

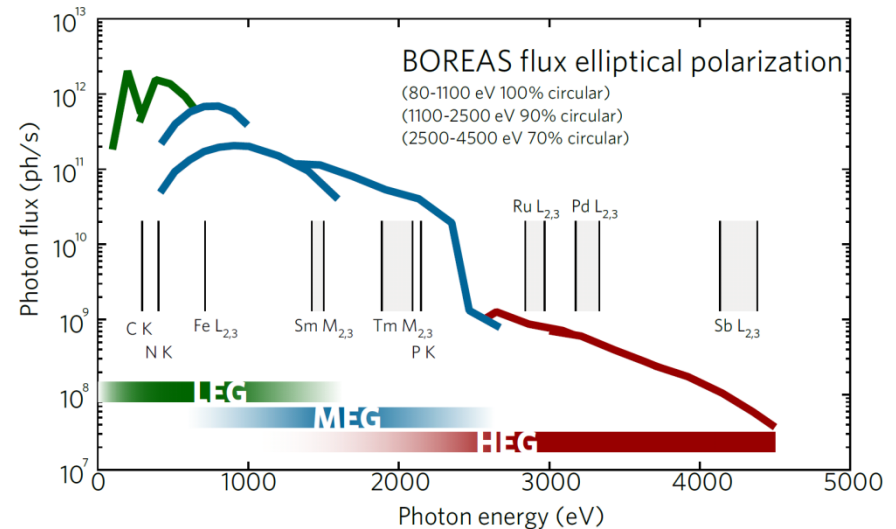


BL highlight:

- **Extended soft X-ray energy range**
- **High flux/High resolving power** (3 gratings x 2 mirror combinations)
- Variable spot size with KB mirror system
- **State-of-art XAS/XMCD/XRS endstation equipment**

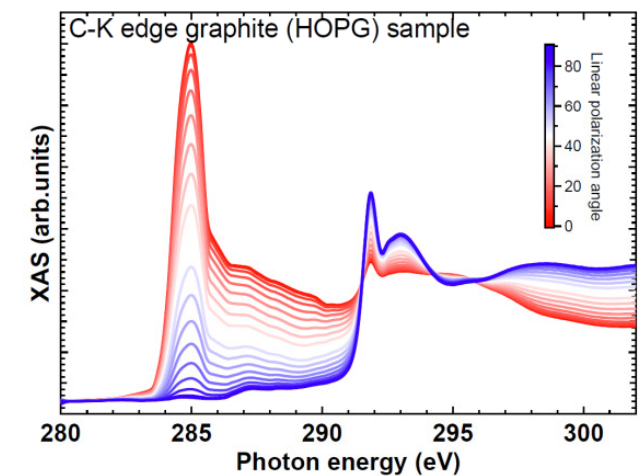
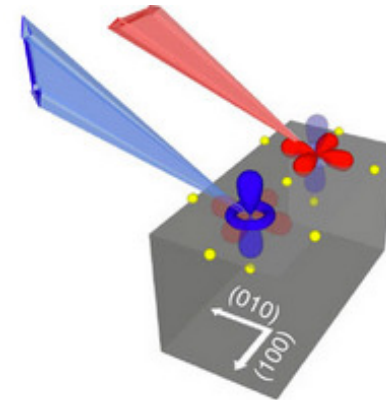
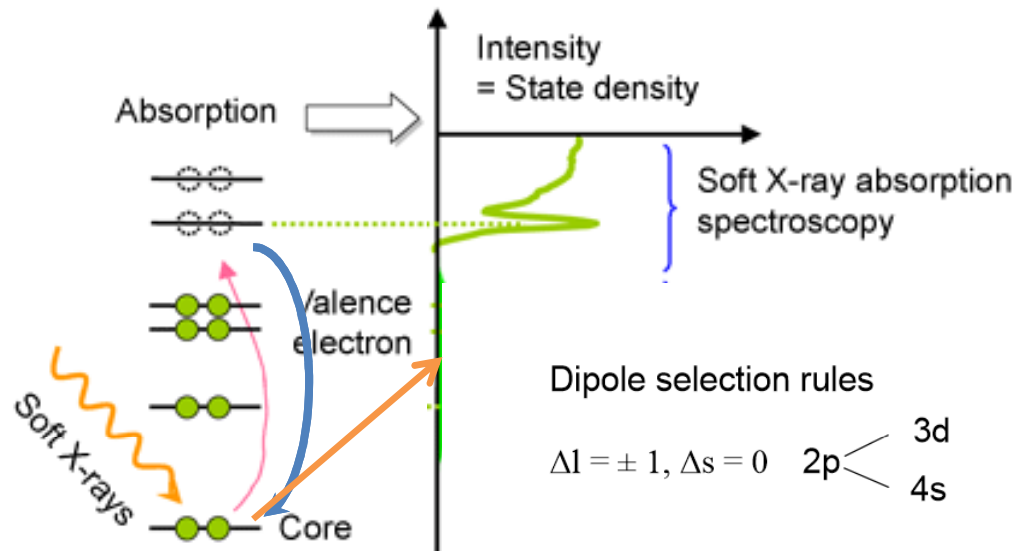


Linear polarization



Circular & elliptical polarization

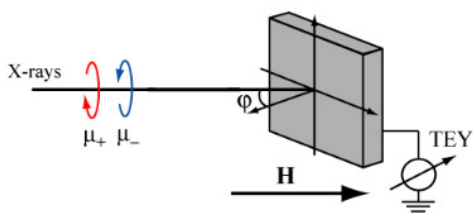
- High flux at optimum resolution (measured at 100mA ring current)
- Considerable flux in the high energy range (>1.5 keV)
- Typically 1st ID harmonic 100-1100 eV ; 3rd : 1000-2500 eV approx. ; 3rd, 5th, ... for E>2000 eV



- XAS chemical sensitivity due to core-level absorption + dipole selection rules
- XAS orbital sensitivity due to light polarization direction
- XRS scattering enhancement in correspondence with intermediate excited state formation → resonant process

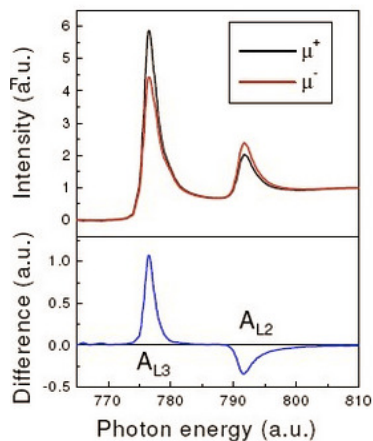


Circular dichroism



Dipole selection rules

3d

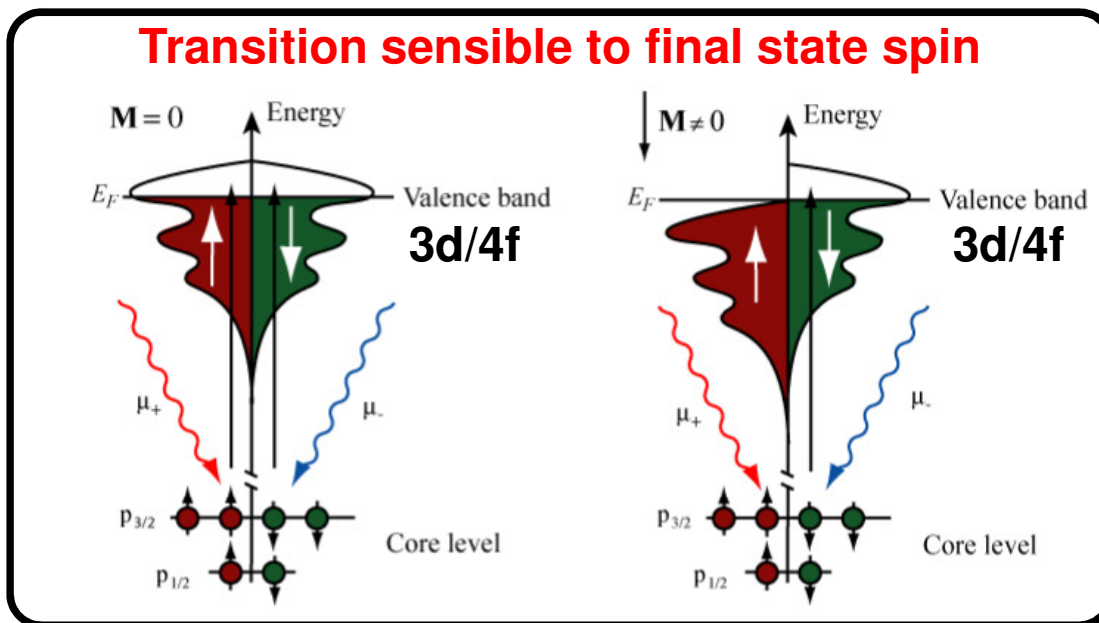


Sum rules

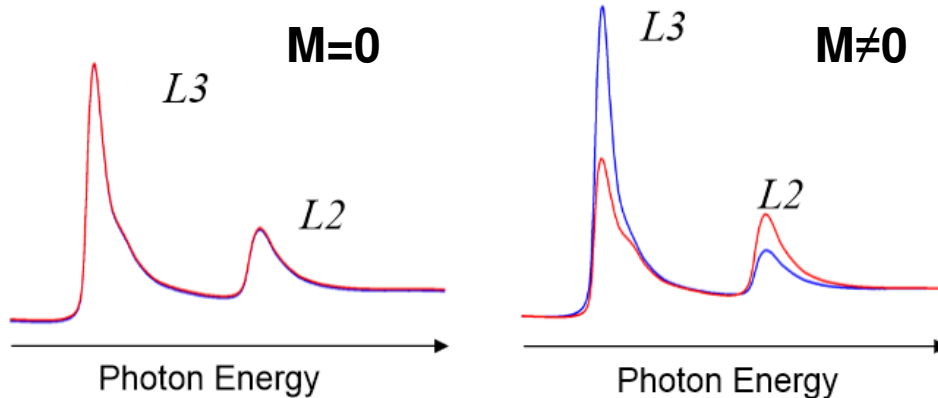
$$m_s/\mu_B \sim \frac{A_{L3} - 2A_{L2}}{A_{iso}}$$

$$m_l/\mu_B \sim \frac{A_{L3} + A_{L2}}{A_{iso}}$$

Transition sensible to final state spin



Absorption spectra





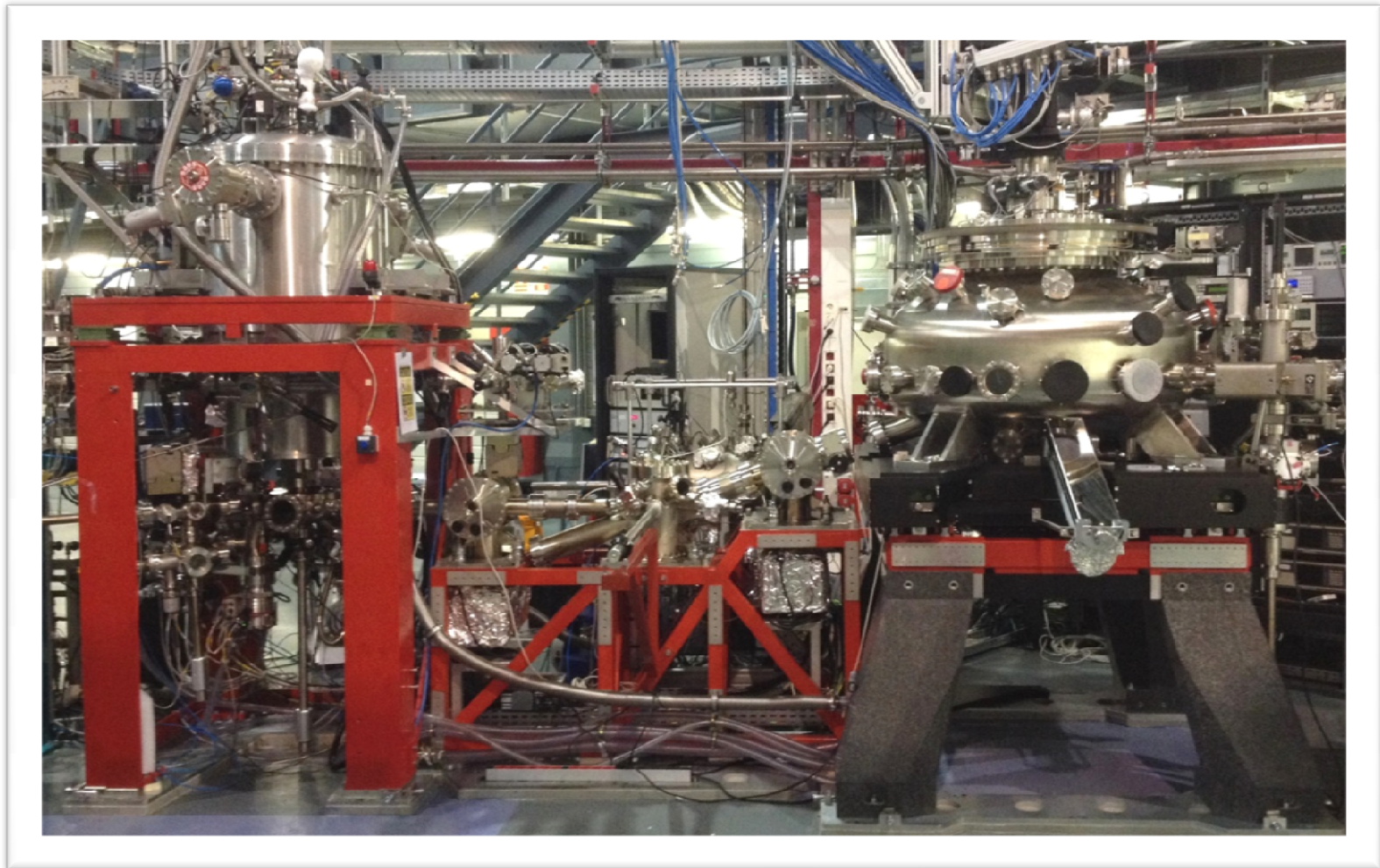
1 H Hydrogen 1.00794																	2 He Helium 4.003
3 Li Lithium 6.941	4 Be Beryllium 9.012182																
11 Na Sodium 22.989770	12 Mg Magnesium 24.3050																
19 K Potassium 39.0983	20 Ca Calcium 40.078	21 Sc Scandium 44.955910	22 Ti Titanium 47.867	23 V Vanadium 50.9415	24 Cr Chromium 51.9961	25 Mn Manganese 54.938049	26 Fe Iron 55.845	27 Co Cobalt 58.933200	28 Ni Nickel 58.6934	29 Cu Copper 63.546	30 Zn Zinc 65.39	31 Ga Gallium 69.723	32 Ge Germanium 72.61	33 As Arsenic 74.92160	34 Se Selenium 78.96	35 Br Bromine 79.904	36 Kr Krypton 83.80
37 Rb Rubidium 85.4678	38 Sr Strontium 87.62	39 Y Yttrium 88.90585	40 Zr Zirconium 91.224	41 Nb Niobium 92.90638	42 Mo Molybdenum 95.94	43 Tc Technetium (98)	44 Ru Ruthenium 101.07	45 Rh Rhodium 102.90550	46 Pd Palladium 106.42	47 Ag Silver 107.8682	48 Cd Cadmium 112.411	49 In Indium 114.818	50 Sn Tin 118.710	51 Sb Antimony 121.760	52 Te Tellurium 127.60	53 I Iodine 126.90447	54 Xe Xenon 131.29
55 Cs Cesium 132.90545	56 Ba Barium 137.327	57 La Lanthanum 138.9055	72 Hf Hafnium 178.49	73 Ta Tantalum 180.9479	74 W Tungsten 183.84	75 Re Rhenium 186.207	76 Os Osmium 190.23	77 Ir Iridium 192.217	78 Pt Platinum 195.078	79 Au Gold 196.96655	80 Hg Mercury 200.59	81 Tl Thallium 204.3833	82 Pb Lead 207.2	83 Bi Bismuth 208.98038	84 Po Polonium (209)	85 At Astatine (210)	86 Rn Radon (222)
87 Fr Francium (223)	88 Ra Radium (226)	89 Ac Actinium (227)	104 Rf Rutherfordium (261)	105 Db Dubnium (262)	106 Sg Seaborgium (263)	107 Bh Bohrium (262)	108 Hs Hassium (265)	109 Mt Meitnerium (266)	110 (269)	111 (272)	112 (277)	113	114				
58 Ce Cerium 140.116	59 Pr Praseodymium 140.90765	60 Nd Neodymium 144.24	61 Pm Promethium (145)	62 Sm Samarium 150.36	63 Eu Europium 151.964	64 Gd Gadolinium 157.25	65 Tb Terbium 158.92534	66 Dy Dysprosium 162.50	67 Ho Holmium 164.93032	68 Er Erbium 167.26	69 Tm Thulium 168.93421	70 Yb Ytterbium 173.04	71 Lu Lutetium 174.967				
90 Th Thorium 232.0381	91 Pa Protactinium 231.03588	92 U Uranium 238.0289	93 Np Neptunium (237)	94 Pu Plutonium (244)	95 Am Americium (243)	96 Cm Curium (247)	97 Bk Berkelium (247)	98 Cf Californium (251)	99 Es Einsteinium (252)	100 Fm Fermium (257)	101 Md Mendelevium (258)	102 No Nobelium (259)	103 Lr Lawrencium (262)				

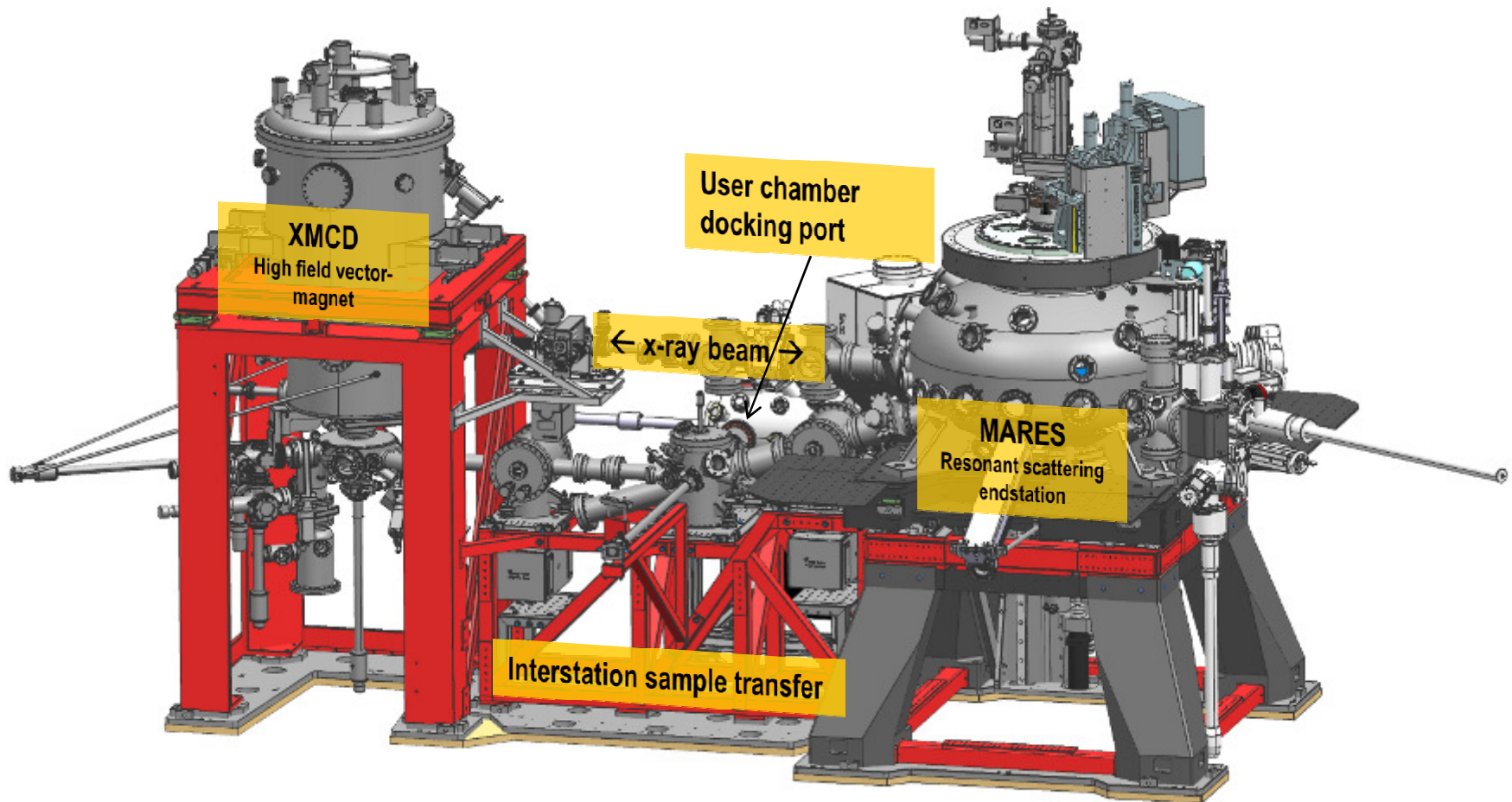
400 – 1000 eV
L2,3 edge 2p->3d

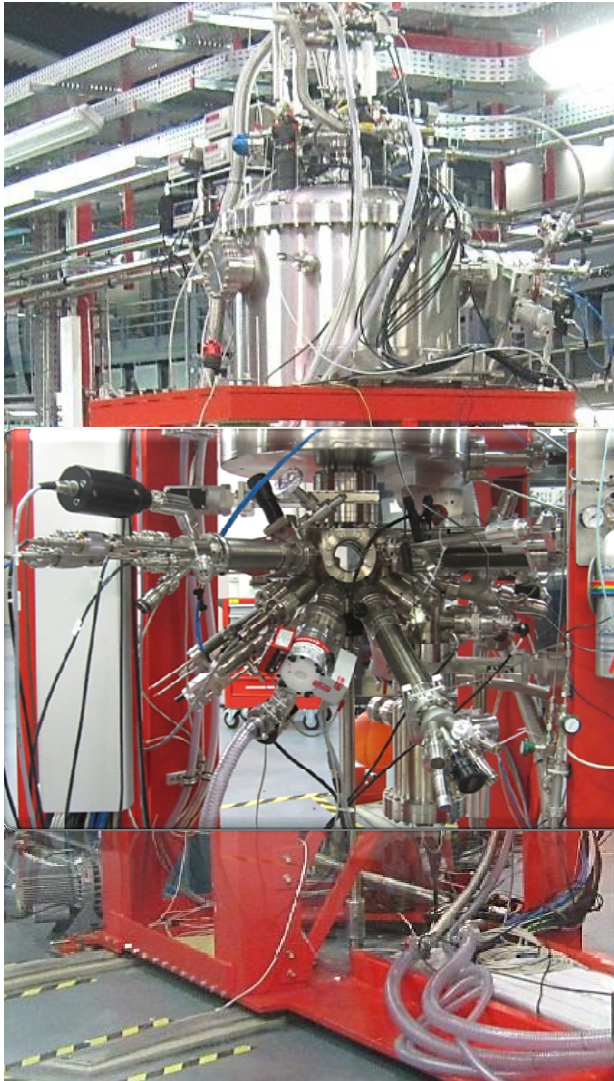
900 – 1600 eV
M 4,5 edge 3d->4f

2300 – 3500 eV
L2,3 edge 2p->4d

180 – 4000 eV
K edge 1s->p/vac.





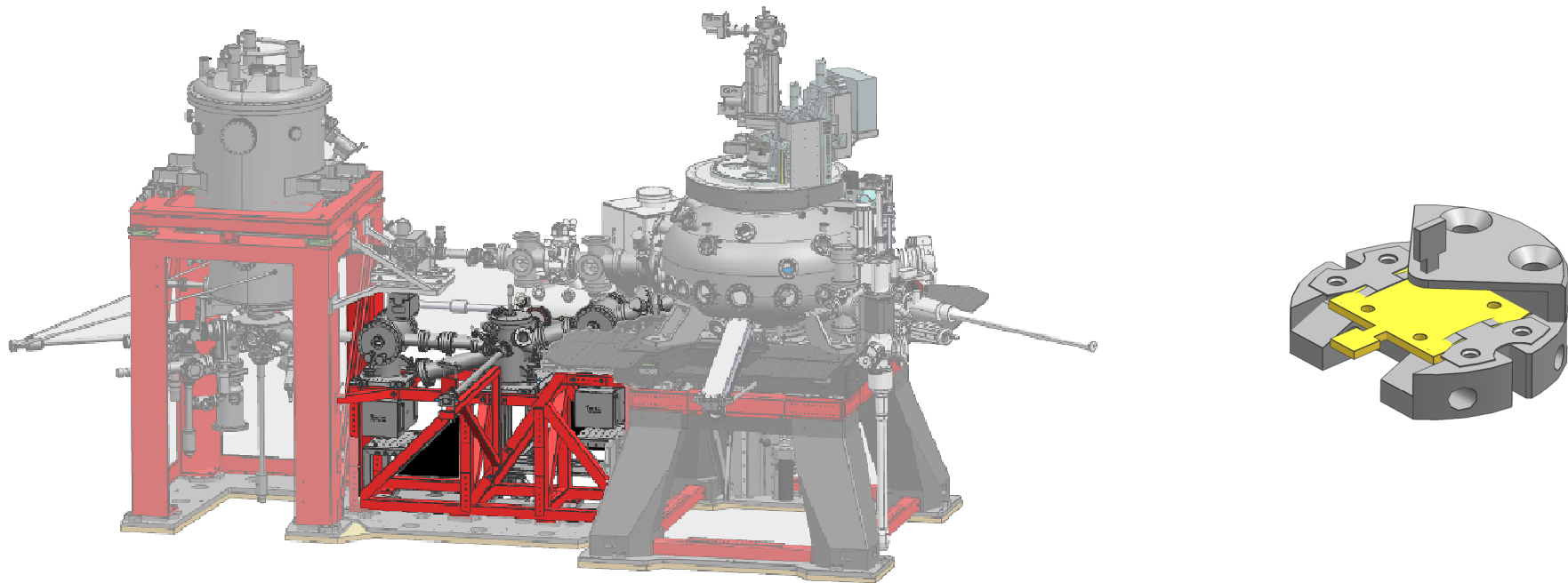


HECTOR – High magnetic field XMCD endstation:

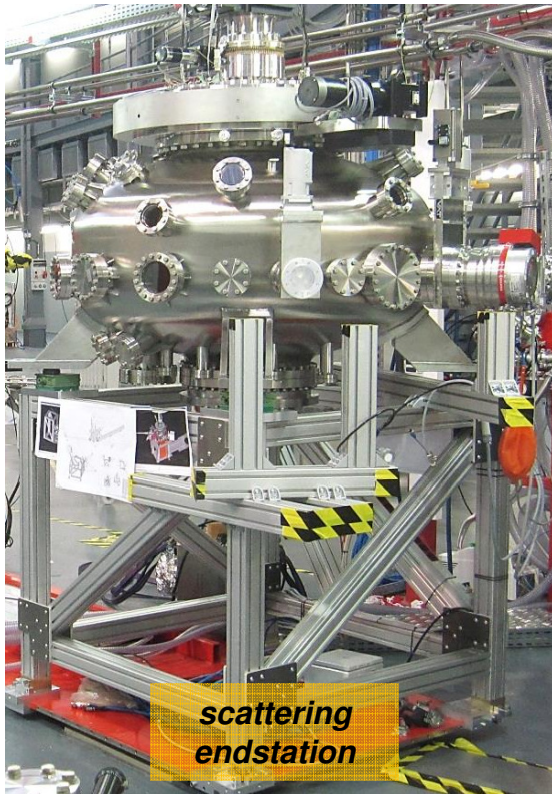
- Up to 6 Tesla along beam
- 2 T sphere mode
- 2-370 K variable sample temperature
- 4 electrical feedthrough available on sample holder
- Signal detection: total electron yield, fluorescence yield and transmission

HECTOR – UHV preparation chamber:

- Fully equipped surface science prep. Chamber: sputtering/annealing, metal/organic evap, mini LEED/AES, quartz balance and fast exchange user equipment
- Cleaver/scrapper for single crystal/pellet
- Fast entry load-lock with up to 4 places + 4 places UHV buffer chamber



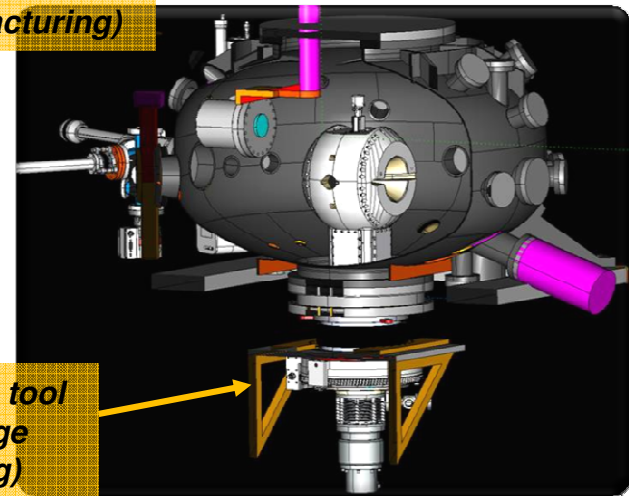
- UHV sample transfer between the two enstation
- Docking port for user-brought chamber/system
- Docking port for smalle UHV “suitcase”
- All compatible with “standard” omicron/specs like sample plates



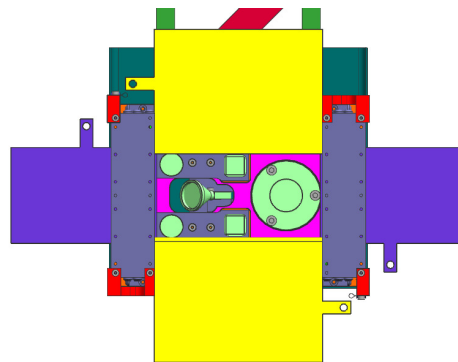
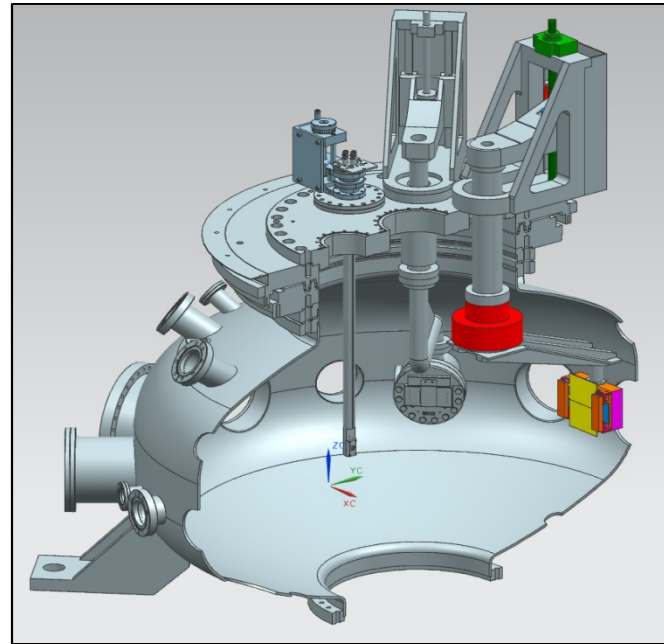
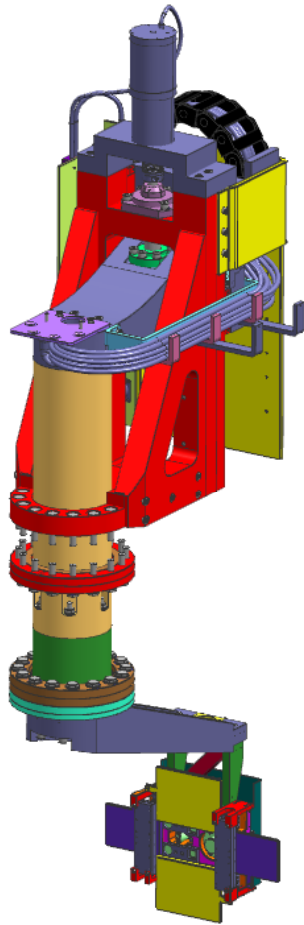
- > Final assembly late 2014
- > Open to users starting from feb. 2015
- > Availability : reflectometry exps. without applied magnetic field

**Two in-vacuum detector arms
(IH-designed, manufacturing)**

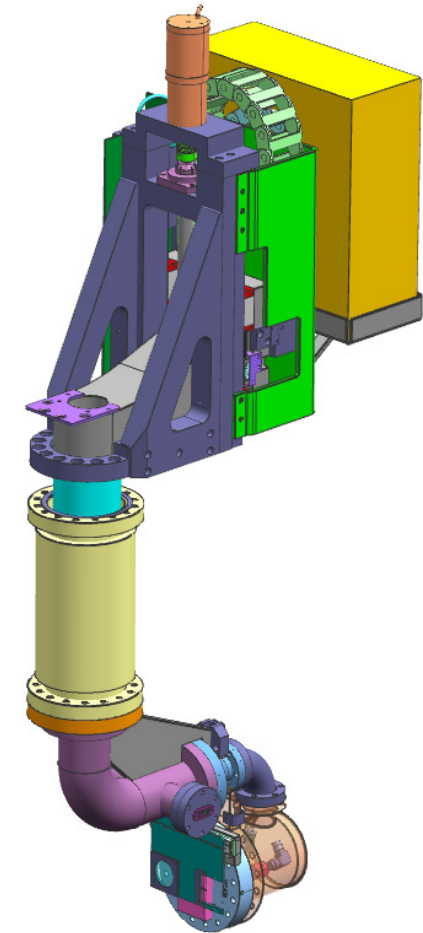
**2 T magnet in/out tool
with rotary stage
(manufacturing)**



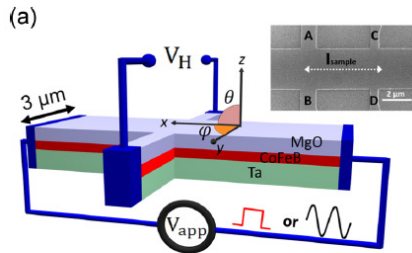
- Surf. science prep chamber (up to now sputtering/annealing stage gas line)
- In-situ deposition with metal/organic molecules evaporator (..with x-ray)
- Variable temperature 17-350 K, 6-DOF sample manipulator
- In-vacuum detector mounted on top rotary stage



> Arm 1 – channeltron,
microchannel plate, diodes, slits



> Arm 2 – XCAM CCD
(SAT OK, june'14)



PHYSICAL REVIEW B 89, 214419 (2014)

Fieldlike and antidamping spin-orbit torques in as-grown and annealed Ta/CoFeB/MgO layers

Can Onur Avci,^{1,2} Kevin Garello,^{1,2} Corneliu Nistor,^{1,2} Sylvie Godey,² Belén Ballesteros,² Aitor Mugarza,² Alessandro Barla,³ Manuel Valvidares,⁴ Eric Pellegrin,⁴ Abhijit Ghosh,¹ Ioan Mihai Miron,⁵ Olivier Boulle,⁵ Stephane Auffret,⁵ Gilles Gaudin,⁵ and Pietro Gambardella^{1,2}

¹Department of Materials, ETH Zurich, Hönggerbergstr. 64, CH-8093 Zürich, Switzerland

²Catalan Institute of Nanoscience and Nanotechnology (ICN2), UAB Campus, E-08193 Barcelona, Spain

³Istituto di Struttura della Materia (ISM), Consiglio Nazionale delle Ricerche (CNR), S.S. 14 Km 163.5, I-34149 Trieste, Italy

⁴ALBA Synchrotron Light Source, E-08290 Cerdanyola del Vallès, Barcelona, Spain

⁵SPINTEC, UMR-8191, CEA/CNRS/UJF/GINP, INAC, F-38054 Grenoble, France

(Received 31 January 2014; revised manuscript received 12 May 2014; published 23 June 2014)

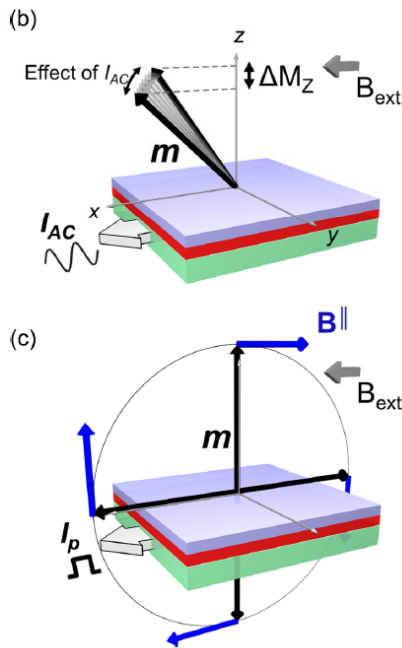
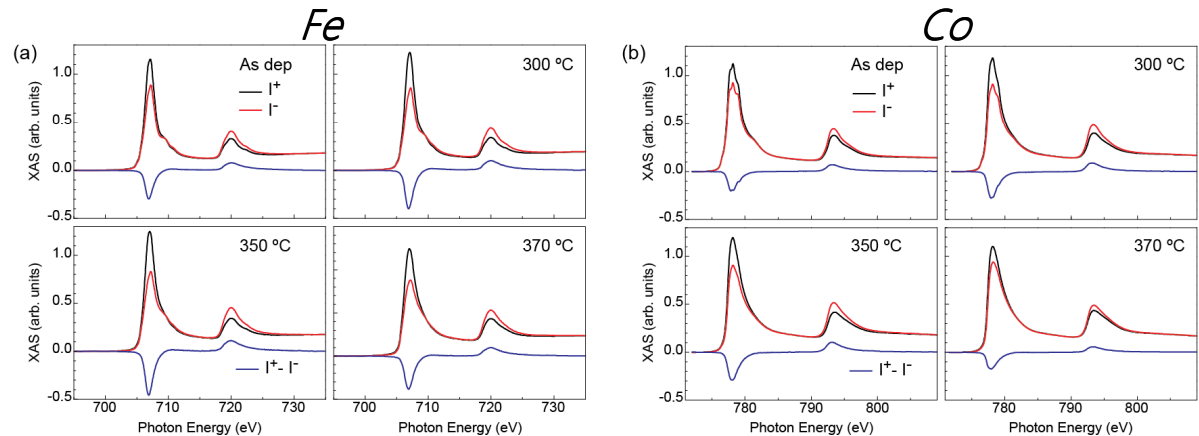
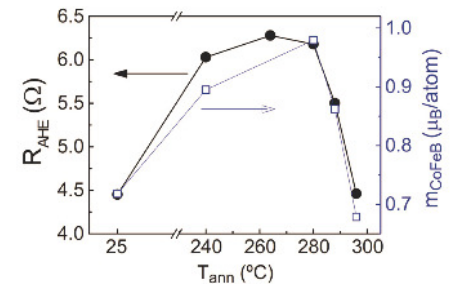


FIG. 2. (Color online) (a) Schematic of the sample and measurement geometry. Inset: Scanning electron micrograph image of a sample. (b) Small oscillations of the magnetization induced by an ac current. (c) Switching of the magnetization induced by the combined action of B^{\parallel} and the external field.



- Element specific magnetic moments measured with XMCD
- Per-atom magnetic moment measured with XMCD applying sum rules analysis



1 Stability of the Cationic Oxidation States in $\text{Pr}_{0.50}\text{Sr}_{0.50}\text{CoO}_3$ across the 2 Magnetostructural Transition by X-ray Absorption Spectroscopy

3 Jessica Padilla-Pantoja,^{*,†} Javier Herrero-Martín,[‡] Pierluigi Gargiani,[‡] Manuel Valdivares,[‡]

4 Vera Cuartero,^{‡,§} Kurt Kummer,[§] Oliver Watson,[§] Nicholas B. Brookes,[§] and José Luis García-Muñoz[†]

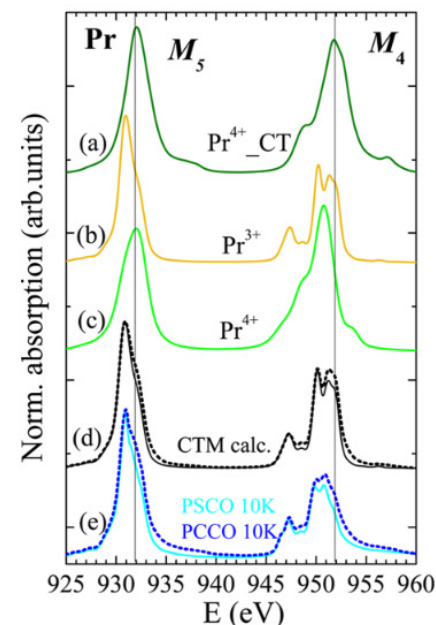
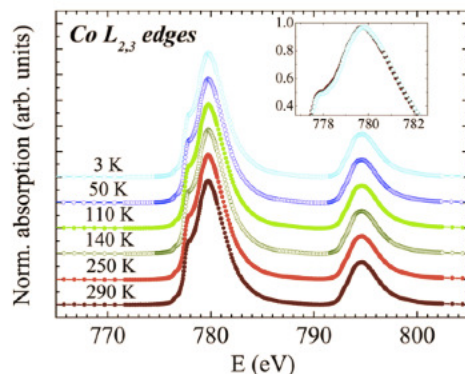
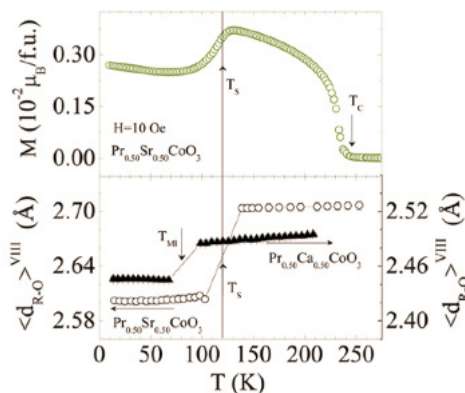
5 [†]Institut de Ciència de Materials de Barcelona (ICMAB)-CSIC, Campus Universitari de Bellaterra, E-08193 Bellaterra, Barcelona, Spain

6 [‡]ALBA Synchrotron Light Facility, 08290 Cerdanyola del Vallès, Barcelona, Spain

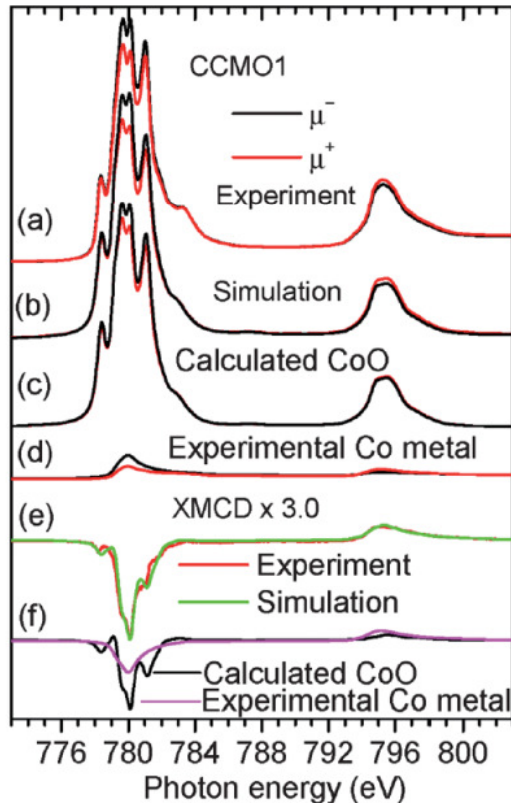
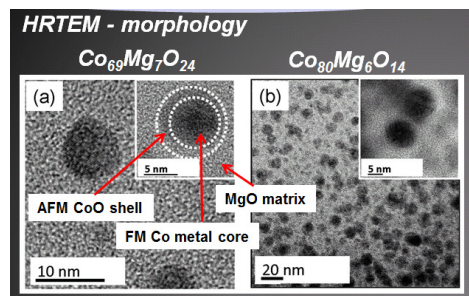
7 [§]European Synchrotron Radiation Facility, F-38043 Grenoble Cedex 9, France

J. Padilla-Pantoja et al (PhD thesis in prep.)

[dx.doi.org/10.1021/ic403117j](https://doi.org/10.1021/ic403117j) | *Inorg. Chem.* 2014, 53, 8854–8858



- Element-specific oxidation state investigation (Co and Pr) via XAS across magneto structural phase transition
- No change in valence of both Co and Pr ions suggests a more complicated mechanism involving LS/HS mixture of Co ions to explain magnetic phase transition



Nanoscale

RSCPublishing

PAPER

View Article Online
View Journal | View Issue

Direct observation of rotatable uncompensated spins in the exchange bias system Co/CoO–MgO

Cite this: *Nanoscale*, 2013, 5, 10236Chuannan Ge,^{ab} Xiangang Wan,^{*a} Eric Pellegrin,^{*c} Zhiwei Hu,^d S. Manuel Valvidares,^c Alessandro Barla,^{ce} Wen-I. Liang,^f Ying-Hao Chu,^f Wenqin Zou^a and Youwei Du^a

We have observed a large exchange bias field $H_E \approx 2460$ Oe and a large coercive field $H_C \approx 6200$ Oe at $T = 2$ K for Co/CoO core-shell nanoparticles (~ 4 nm diameter Co metal core and CoO shell with ~ 1 nm thickness) embedded in a non-magnetic MgO matrix. Our results are in sharp contrast to the small exchange bias and coercive field in the case of a non-magnetic Al_2O_3 or C matrix materials reported in previous studies. Using soft X-ray magnetic circular dichroism at the Co-L_{2,3} edge, we have observed a ferromagnetic signal originating from the antiferromagnetic CoO shell. This gives direct evidence for the existence of rotatable interfacial uncompensated Co spins in the nominally antiferromagnetic CoO shell, thus supporting the uncompensated spin model as a microscopic description of the exchange bias mechanism.

Received 23rd April 2013

Accepted 27th July 2013

DOI: 10.1039/c3nr02013d

www.rsc.org/nanoscale

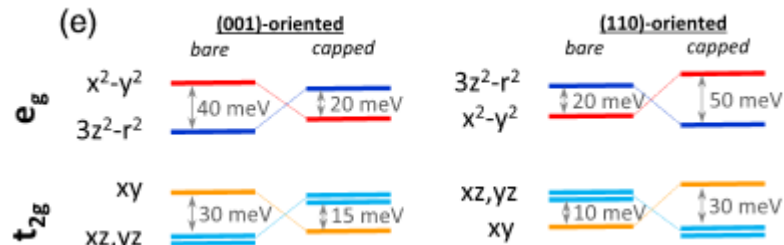
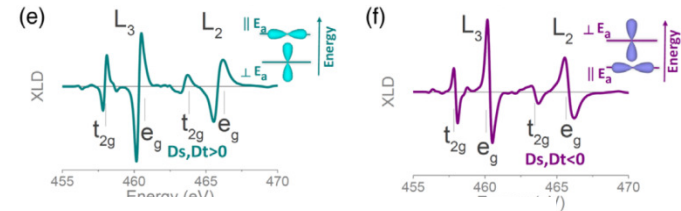
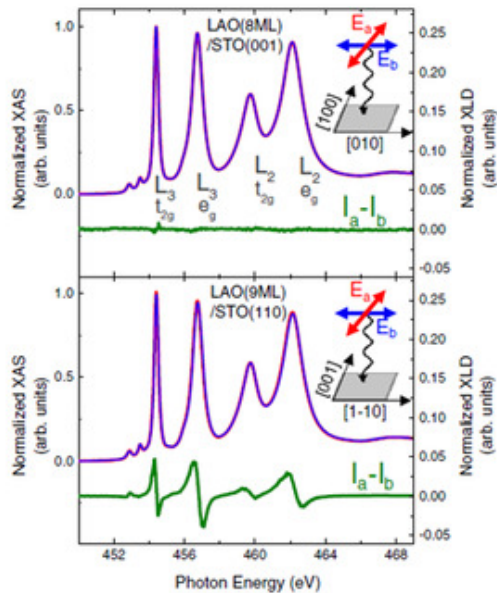
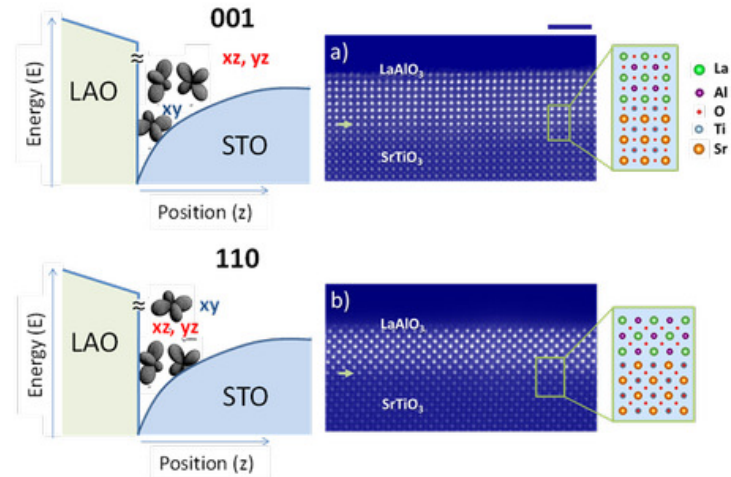
Separation of different dichroic contribution with exp/simulation comparison:

- Uncompensated rotatable Co^{2+} spins in nominally AFM CoO shell stabilized by MgO matrix.
- Metallicity cancels CoO FM contribution
- 30% Co metal + 70% ferromagnetic Co^{2+} in dichroic spectrum.
- Larger part of ferromagnetic signal stems from CoO shell

Two-Dimensional Electron Gases at LaAlO₃/SrTiO₃ Interfaces: Orbital Symmetry and Hierarchy Engineered by Crystal Orientation

D. Pesquera,¹ M. Scigaj,^{1,2} P. Gargiani,³ A. Barla,⁴ J. Herrero-Martín,³ E. Pellegrin,³ S. M. Valvidares,³ J. Gázquez,¹ M. Varela,^{5,6} N. Dix,¹ J. Fontcuberta,¹ F. Sánchez,¹ and G. Herranz,^{1,2}
¹Institut de Ciència de Materials de Barcelona (ICMAB-CSIC), Campus de la UAB, Bellaterra E-08193, Catalonia, Spain
²Departamento de Física, Universitat Autònoma de Barcelona, E-08193 Bellaterra, Barcelona, Catalonia, Spain
³ALBA Synchrotron Light Source, Carretera BP 1413 km 3.3, E-08290 Cerdanyola del Vallès, Barcelona, Spain
⁴Istituto di Struttura della Materia, ISM CNR, Area Science Park Basovizza (Ts), Trieste I-34149, Italy
⁵Departamento Física Aplicada III, Universidad Complutense de Madrid, Madrid, 28040 Spain
⁶Materials Science and Technology Division, Oak Ridge National Laboratory, Oak Ridge, Tennessee 37831, USA
 (Received 9 May 2014; revised manuscript received 24 July 2014; published 7 October 2014)

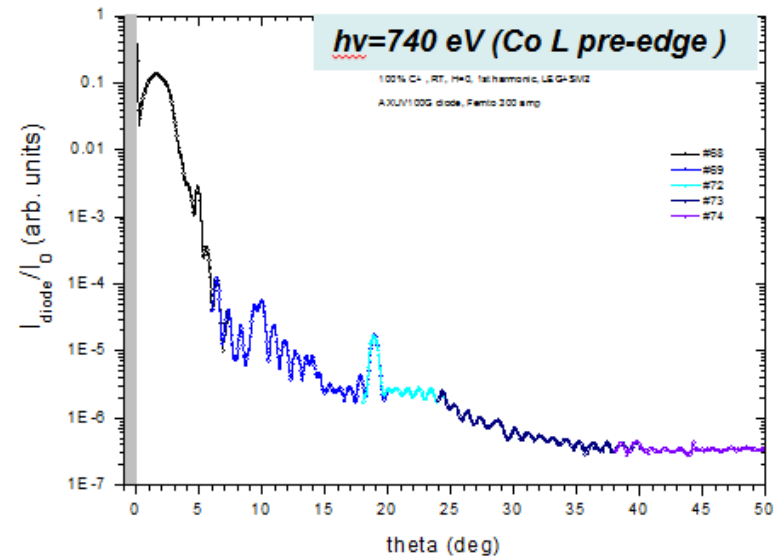
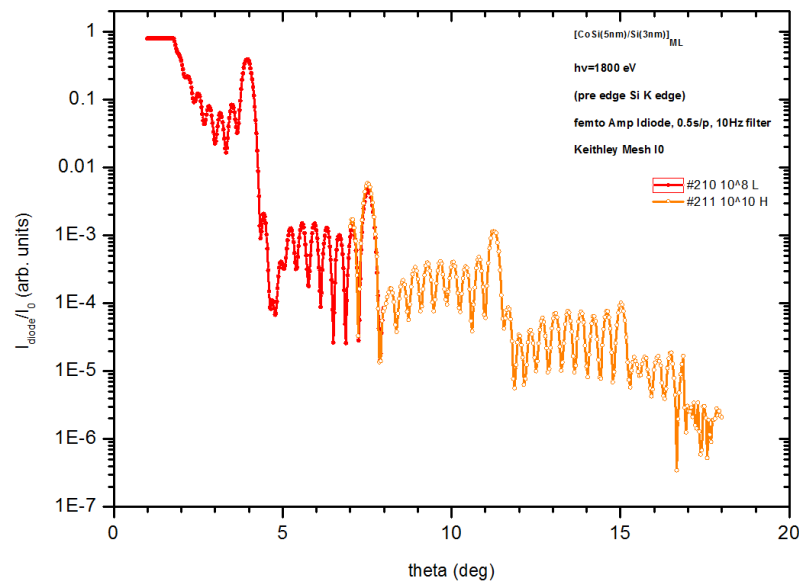
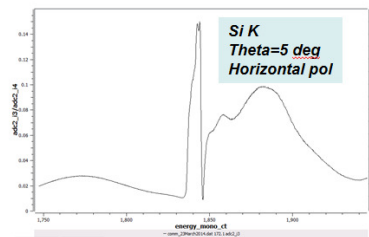
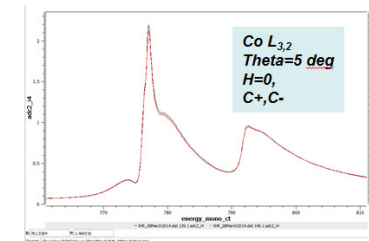
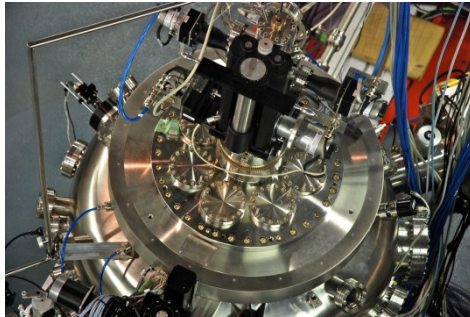
Recent findings show the emergence of two-dimensional electron gases (2DEGs) at LaAlO₃/SrTiO₃ interfaces along different orientations; yet details on band reconstructions have remained so far unknown. Via x-ray linear dichroism spectroscopy, we demonstrate that crystal symmetry imposes distinctive 2DEG orbital hierarchies on (001)- and (110)-oriented quantum wells, allowing selective occupancy of states of different symmetry. Such orientational tuning expands the possibilities for electronic engineering of 2DEGs and opens up enticing opportunities to understand the link between orbital symmetry and complex correlated states at LaAlO₃/SrTiO₃ quantum wells.



- LAO/STO interface crystal orientation dependent orbital hierarchy resolved by XLD at Ti L_{2,3} edge
- High resolution/high energy reproducibility needed to perform such experiment

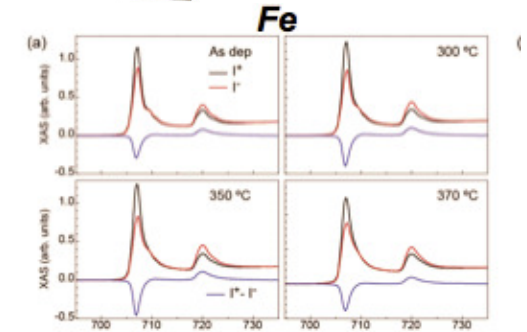
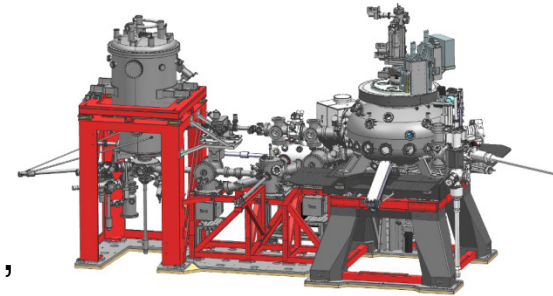


[CoSi(5nm)/Si(3nm)] Multilayer test sample reflectivity
 March 2013 in-house/commissioning time
 Diode detector mounted on a “temporary” support

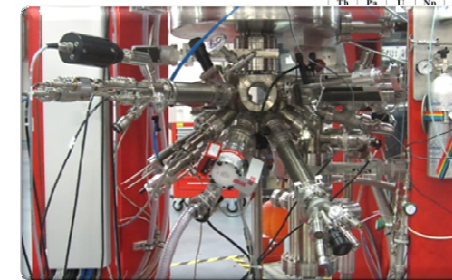


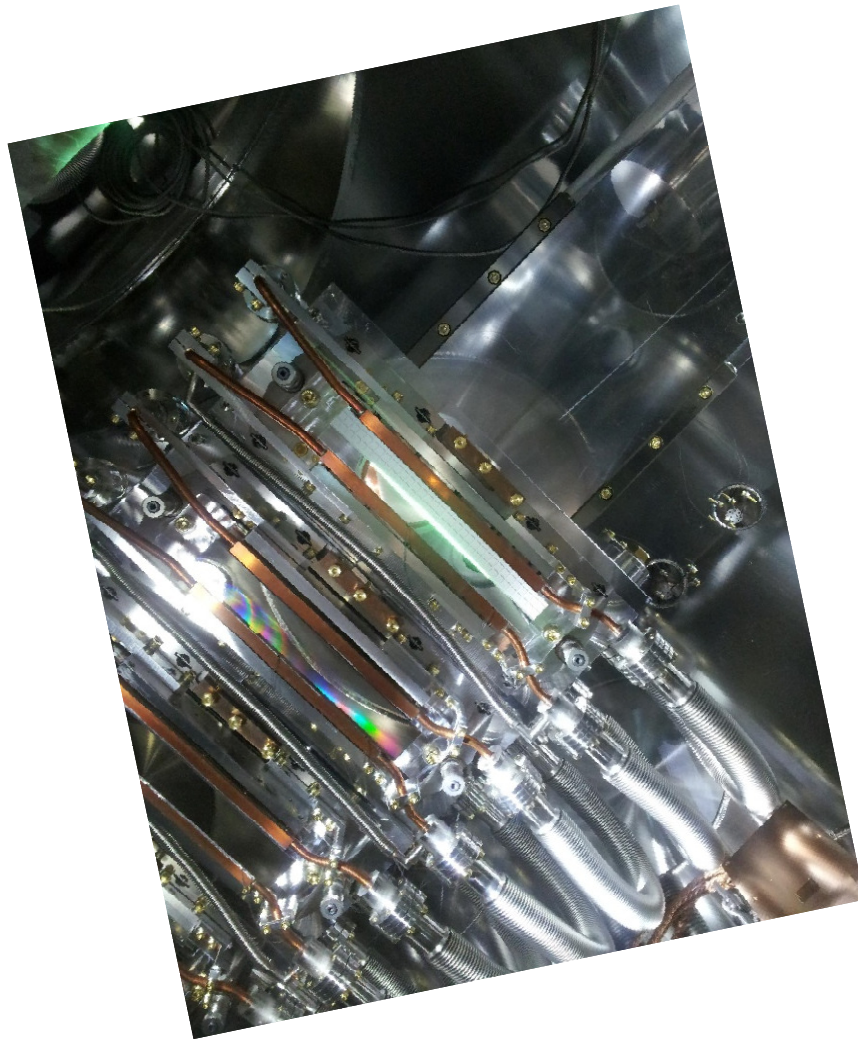
ALBA Remarks

- Two endstation beamline for **X-ray absorption**, **magnetic circular dichroism** and **X-ray magnetic resonant scattering**
- **Element specific magnetic properties**: orbital/spin moment, magnetic anisotropy
- X-ray resonant magnetic scattering experiment for element specific magnetic/structural properties
- Peculiar energy range allowing **4d elements magnetic studies** and **intermediate K-edge elements** (**Sulphur, Calcium..**)
- Very good instrumentation available for sample preparation and surface science experiments



1	H	1.00794	2	He	4.002602
3	Li	6.941	4	Be	9.012182
5	B	10.811	6	C	12.010738
7	N	14.006432	8	O	15.999032
9	F	18.9984032	10	Ne	19.992479
11	Na	22.98976928	12	Mg	24.3046888
13	Al	26.9815386	14	Si	28.0855836
15	P	30.973761998	16	S	32.065
17	Cl	35.453	18	Ar	39.9481634
19	K	39.09831	20	Ca	40.078
21	Sc	44.955912	22	Ti	47.88
23	V	50.9415	24	Cr	51.9961
25	Mn	54.938045	26	Fe	55.845
27	Co	58.933195	28	Ni	58.6934
29	Cu	63.546	30	Zn	65.38
31	Ga	69.723	32	Ge	72.630
33	As	74.9216	34	Se	78.96
35	Br	79.904	36	Kr	83.80
37	Rb	85.4678	38	Sr	87.62
39	Y	88.905848	40	Zr	91.224
41	Nb	92.90638	42	Mo	95.94
43	Tc	98.90625	44	Ru	101.07
45	Rh	102.90550	46	Pd	106.42
47	Ag	107.8682	48	Cd	112.414
49	In	114.818	50	Sn	118.710
51	Sb	121.757	52	Te	127.60
53	I	126.90509	54	Xe	131.29
55	Cs	132.90545196	56	Ba	137.327
57	La	138.90471	58	Ce	140.90764
59	Pr	140.90764	60	Nd	144.2427
61	Pm	144.91288	62	Sm	150.36
63	Eu	151.964	64	Gd	157.25
65	Tb	158.92532	66	Dy	162.50
67	Ho	164.93032	68	Er	167.259
69	Tm	168.93032	70	Yb	173.054
71	Lu	174.96706	72	Hf	178.49
73	Ta	180.94788	74	W	183.84
75	Re	186.207	76	Os	190.23
77	Ir	192.222	78	Pt	195.084
79	Au	196.966569	80	Hg	200.59
81	Tl	204.3833	82	Pb	207.2
83	Bi	208.980389	84	Po	209
85	At	210	86	Rn	222
87	Fr	223	88	Ra	226
89	Ac	227	90	Th	232.0377
91	Pa	231.036888	92	U	238.02891
93	Np	237.048173	94	Pu	244.06422
95	Am	243.061381	96	Cm	247
97	Bk	247	98	Cf	251
99	Es	252	100	Fm	257
101	Md	258	102	No	259
103	Lr	262	104	Uu	289
105	Uu	289	106	Uu	289
107	Uu	289	108	Uu	289
109	Uu	289	110	Uu	289
111	Uu	289	112	Uu	289
113	Uu	289	114	Uu	289
115	Uu	289	116	Uu	289
117	Uu	289	118	Uu	289
119	Uu	289	120	Uu	289





BL29 Staff

M. Valvidares, J. Herrero (BL scientists), H. Babu (BL postdoc)
 J. Moldes (controls), A. Crisol (eng.), F. Farre (tech.), J. Prieto (tech.)
 X. Fariña and X. Serra (electronics)

Special ALBA contributors

E. Pellegrin, S. Ferrer, C. Colldelram, J. Nicolas, D. Fernandez, G. García, M. A. García-Aranda, L. Campos, User Office

Former staff & technical help

A. Barla, R. Martin, J.F. Moreno, D. Bacescu, J. C. Martinez, J. Lidon, O. Matilla, S. Rubio, Fulvio, J. Navarro, C. Ruget, Alex, Paco, Lluís, Eshraq, Xavi P., C. Orozco, D. Iriarte, Thiago, A. Ruz,, S. Astorga, Bern, Oscar, David, J. Ferrer, legal section (CFTs)

Externals: J. B. Kortright, N. Brookes, J. Criginski, C. Quiros, J. M. Alameda, C. Piamonteze, T. Schroder

External companies

TOYAMA, SCI-MAG, CVT, VG, HTS-110, PINK, SPECS, DODECON, FERROVAC, GAMMVAC, TECNOVAC, VAT, IBERLASER, HOSITRAD, VCS, AVS, AVACTEC, VAQTEC, MCALLISTER, HAMAMATSU, XCAM, AMBAR, INSERTY, SPARK, NANOTEC, SJUTS, KONIK, MDC, TRINOS, VAT